64-8

(5) 39,950

(1)

TR-1106

FLUID AMPLIFICATION

7. A Three – Stage Digital Amplifier

Carl J. Campagnuolo

1 August 1963

HARRY DIAMOND LABORATORIES
FORMERLY: DIAMOND ORDNANCE FUZE LABORATORIES
ARMY MATERIEL COMMAND
WASHINGTON 25, D.C.

Distributed by the Office of Technical Services
U.S. Department of Commerce, Washington 25, D.C.

$1.00

HARRY DIAMOND LABORATORIES

Robert W. McEvoy
LtCol, Ord Corps
Commanding

B. M. Horton
Technical Director

MISSION

The mission of the Harry Diamond Laboratories is:

(1) To perform research and engineering on systems for detecting, locating, and evaluating targets; for accomplishing safing, arming, and munition control functions; and for providing initiation signals: these systems include, but are not limited to, radio and non-radio proximity fuzes, predictor-computer fuzes, electronic timers, electrically-initiated fuzes, and related items.

(2) To perform research and engineering in fluid amplification and fluid-actuated control systems.

(3) To perform research and engineering in instrumentation and measurement in support of the above.

(4) To perform research and engineering in order to achieve maximum immunity of systems to adverse influences, including countermeasures, nuclear radiation, battlefield conditions, and high-altitude and space environments.

(5) To perform research and engineering on materials, components, and subsystems in support of above.

(6) To conduct basic research in the physical sciences in support of the above.

(7) To provide consultative services to other Government agencies when requested.

(8) To carry out special projects lying within installation competence upon approval by the Director of Research and Development, Army Materiel Command.

(9) To maintain a high degree of competence in the application of the physical sciences to the solution of military problems.

391950

UNITED STATES ARMY MATERIEL COMMAND
HARRY DIAMOND LABORATORIES
WASHINGTON 25, D.C.

Proj.
DA-1P010501A001
~~AMCMS Code 5011.11.71200~~
HDL Proj 31131

HDL

TR-1106

1 August ~~1963~~,

FLUID AMPLIFICATION

7. A Three-Stage Digital Amplifier,

by Carl J. Campagnuolo,

(UPPER CASE)

FOR THE COMMANDER
Approved by

Robert D. Hatcher
R. D. Hatcher
Chief, Laboratory 300

WJB

CONTENTS

ILLUSTRATIONS

Figures

ABSTRACT

The design and performance of a three-stage digital amplifier system obtaining a high-power output and flow gain is described. The design of the system was arrived at by taking measurements of single elements and matching the units with respect to input, output, and feedback performance. Flow gain in the system was obtained by increasing the nozzle widths by a factor of ten from stage to stage. Effects of loading on the stability of intermediate units were controlled by positioning the splitters further downstream than would be required for maximum efficiency.

The system was operated with a common power-jet supply pressure of 1 to 15 psig. The system was switched with flow at atmospheric pressure. The third-stage output was exhausted to atmosphere through a 12-deg diffuser. Flow gains up to 3000, pressure recovery of 50 to 67 ~~percent~~ %, and power gains up to about 10,000 were obtained.

1. INTRODUCTION

One of the basic elements of fluid amplification is the boundary-layer digital unit. The purposes of this paper are to discuss some of the design parameters of such units making up a three-stage digital system with a high flow gain and a reasonable pressure recovery, and to present measurements made on two experimental cascaded systems.

A boundary-layer unit works on principles some of which have not yet been completely explained by classical fluid dynamics. The most important of these are wall-jet interaction and entrainment of fluid particles from the surroundings (ref 1). Although a boundary-layer unit can operate in all three ranges of flow—subsonic, transonic, and supersonic—this paper is primarily concerned with units operated in the subsonic range.

2. PRINCIPLES OF OPERATION

When a jet exhausts from a nozzle, turbulence is generated at the borders of the jet. Due to friction from shearing stresses against the surrounding fluid, the jet undergoes lateral diffusion and deceleration, and, at the same time, fluid particles are entrained by the jet (ref 2). As the surrounding fluid mixes with the jet, the velocity distribution of the jet changes, so that the velocity profile approaches a Gaussian distribution at a distance of about 6 w (nozzle widths). During the diffusion process, the kinetic energy of the jet transforms into kinetic energy of turbulence, which in turn is converted into heat energy. In this process, the jet is decelerated while the surrounding particles are accelerated. This results in a net increase in the output flow. Even though the velocity of most of the jet decreases with distance from the nozzle, there is a zone called the core within about 6 w from the nozzle where the velocity is maximum and constant (ref 2). The highest

energy of the jet is in the core region, since no mixing with the outside has yet taken place.

2.1 Digital Characteristics

The digital character of the boundary-layer unit is obtained by providing walls or fixed boundaries adjacent to the jet (fig. 1). The jet emerging from the power nozzle attaches to one of the walls forming a low-pressure pocket or bubble. The trajectory of the jet around the low-pressure bubble is approximately the arc of a circle. The pressure within the bubble varies with distance from the nozzle because particles are constantly being taken away and returned by the main stream. The pressure in the bubble must be increased by flow from the control nozzle before the jet will detach from the wall and attach to the opposite wall. This is one of the factors responsible for the digital characteristic of these elements.

The static pressure distribution on the wall with the jet attached is mostly a function of the setback and angle of inclination of the wall, varying from below ambient up to a maximum and then dropping slowly until, at a long distance from the nozzle, it approaches ambient. A typical static pressure distribution along an attachment wall is shown in figure 2.

2.2 Jet-Edge Oscillations

It is well known from classical aerodynamics that the presence of a wedge (splitter) in a stream will cause the jet to oscillate as was first observed by C. Sondhaus (ref 3) and R. Wachmuth (ref 4). Consequently, the presence of the splitter gives rise to resonant frequencies with associated harmonics, the cause and magnitude of which have been the subject of numerous investigations. This phenomenon increases the noise level of the unit and the resulting losses significantly decrease efficiency. The oscillations are decreased by rounding the wedge.

2.3 Efficiency

A most important consideration in building digital units is efficiency; i.e., there should be only a small loss of the total energy of the power jet. In data due to Albertson (ref 2) for free jets in the atmosphere, it is evident that the total energy decreases with distance. From the same data, it is also evident that up to a distance of 6 w, the maximum velocity in the direction of the jet flow is constant; and it decreases exponentially farther downstream. From such information, one may conclude that to construct efficient units, it is necessary to maintain the expansion chamber of the jet as small as possible and have the divider no farther downstream than 6 w.

The stream can be diffused very efficiently with a 12-deg diffuser to obtain a high pressure efficiency. The diffuser must be kept short to minimize losses. Elements fulfilling these requirements have been built; pressure recovery of about 70 percent and instantaneous flow gains greater than 15 have been achieved in the subsonic range with up to 15 psig power-jet supply pressure. (By pressure recovery is meant the amount of loading that the unit can sustain, measured in terms of the stagnation pressure at the power-jet input.

2.4 Switching Characteristics

A digital unit that is designed for a high-pressure efficiency is sensitive to rather small signals applied at the controls. In other words, it is easy to change the position of the stream from one channel to the other, and the energy expended in this process is small. Actually, in some elements, atmosphere can supply sufficient flow and pressure to switch the output. This is possible because the pressure in the jet-inclosed bubble is only 9 to 12 psia, and the ambient (atmospheric) pressure is over 14 psia. Consequently, if the control port is opened, flow will enter from the atmosphere, the pressure in the bubble will increase, and the jet will attach to the opposite wall.

2.5 Stability and Memory

Unfortunately, an efficient subsonic digital element works well only as long as no load is present in its output. If a small load such as another unit is present at the output, the static pressure at the output increases, and this pressure propagates upstream shifting the point of attachment upstream. This shrinks the entrainment bubble, and its pressure also increases. The stream will then shift to the other channel, or, in some designs, will oscillate between the two channels. Such effects are very undesirable if the unit must operate into a load.

Memory is obtained when the splitter is moved sufficiently downstream to allow the stream to turn and exhaust out the opposite outlet without creating turbulence at the attachment point. The stream remains attached to the wall even with the output of the amplifier completely blocked. The flow will exhaust from the opposite channel, but the pressure will remain in the blocked channel. If the blocked channel is reopened, the stream will exhaust from that channel. Memory is very important in the driver of a bistable cascaded system.

2.6 Feedback in Cascaded Systems

Positive feedback loops may be present when two units are coupled. The feedback loop arises from the motion of fluid particles

from the next stage interacting with the main stream. This process can best be explained by considering figure 3, which shows three units connected together. The shaded region is the region of flow. In leg 1, the pressure is lowered since the stream in the third stage is continually entraining particles. At the same time, the power stream in the second stage also entrains particles from leg 2. If the two pressures are approximately equal, then the feedback is approximately zero. If leg 2 is at a lower pressure than leg 1, there will be counter flow, that is, feedback.

3. THREE -STAGE DIGITAL AMPLIFIERS

Two three-stage digital amplifier systems were fabricated and tested. One system consisted of three digital elements connected together by flexible hoses with the outputs of the first and second stages exhausting directly into the second and third stages, respectively. This system was designed empirically by testing single elements to determine their performance and then matching the units to obtain the desired system performance. The system is shown schematically in figure 3.

The second system was designed as an integral three-stage unit using the first system as a design reference and adjusting parameters as test performance of the first system indicated would be desirable. The first and second stages of the system were exhausted via vortex cylinders to succeeding stages. The vortex cylinder acts as an impedance matching device. A schematic of the integral system is shown in figure 4. Design drawings of the unit are shown in figures 5, 6, and 7. A photograph of the unit is given in figure 8.

The width of the control nozzle was the same as that of the power-jet nozzle in any given stage in both systems. In both systems, the areas of the power-jet nozzle were increased by a factor of ten from stage to stage to obtain the flow and power gain. Specifically, the nozzle areas were 0.001, 0.01, and 0.1 $in.^2$; the aspect ratios of the third stage power jets were 4:1. In the third stage of both systems, the attachment wall angle was 12 deg, and the wall offset was zero.

The pressure efficiency of the first and second stages was sacrificed in positioning the splitters at a distance of 16 w from the nozzle in the first stage and 8 w in the second, with 4 w in the third. This splitter arrangement was necessary to obtain stability and memory in the driver and intermediate stage.

The apparatus used to determine the characteristics of the individual units which make up the first system is shown in figure 9. The pressures at the inputs and outputs of the single units were measured by means of transducers; the input and output flows were measured

directly by flowmeters and also computed from the pressure differences measured across orifice plates. The signal outputs from the transducers were plotted on an x-y recorder. Plots were obtained directly by changing the input pressure continuously with a motorized valve. Once the characteristics of the individual elements were known, it was a simple matter to match them together to obtain the desired system performance.

Figures 10 and 11 show the apparatus used to measure the pressure distribution along the attachment wall. The static taps were placed one nozzle width apart along the wall. With this apparatus, it was possible to find the point of attachment of the jet and also to determine its movement as some of the parameters were varied. The pressure distribution was measured using manometers. Typical data are shown in figure 2.

3.1 Performance of the Three-Unit Digital Amplifier System

Performance of the three-unit digital cascade was determined using the test setup shown in figures 12 and 13. Pitot tubes surrounded by static pressure tap holes (fig. 14) were placed in each leg of the system to determine the static and dynamic pressure in the output of each stage. The system was tested with a common power-jet supply pressure for the three stages. This pressure was varied from 1 to 14 psig.

Static pressure in the outputs is plotted in figure 15. Total pressure in the outputs is plotted in figure 16. The Mach number in the second and third stage outputs is plotted in figure 17.

Figure 15 shows that the static pressure is highest in the second-stage output, which indicates that the control nozzle of the third stage is the smallest with respect to available flow. The static pressure is least at the output of the third stage since the unit is exhausting into the atmosphere. The static pressure in the first-stage output is also relatively high indicating the second-stage control nozzle is also relatively small with respect to flow.

The total pressure is relatively low in the third-stage output since the measurements were made considerably further downstream than in the first and second stages. It may be noted that the total pressure in the first stage output is almost all static, hence, that the fluid velocity is very slow.

3.2 Performance of Integral Three-Stage Digital Amplifier

The integral three-stage amplifier is shown in figures 4 through 8. Design of the stages was the same as the design of the elements in the three-unit cascaded system except that the first- and second-stage outputs are exhausted to control nozzles via the vortex cylinders. The performance of the unit was determined using a test setup schematically the same as that shown in figure 14 except that the static and

total pressure in the outputs of the first and second stages were not measured being inaccessible because of the integral construction. In the performance tests, a common power-jet supply pressure was used for all stages.

The unit output entered a tank and, thence, through a gate valve and flowmeter, as shown in figure 18, before being exhausted to the atmosphere. The pressure recovery of the unit was measured by closing the gate valve. When the valve was partly closed thereby loading the output of the third stage, some of the dynamic pressure of the stream was transformed into static pressure in the tank, which was measured with the gage connected to it. As the valve was being closed, the static pressure built up in the upper portion of the diffuser in the third stage. When the pressure became equal to that at the entrance to the diffuser, resonant effect caused oscillations. As closing of the gate valve was continued, the resonant effect was eliminated.

Two curves of pressure recovery as a ratio of the output static pressure with loading to the common power-jet supply pressure are presented in figure 19, with the supply pressure varied from 1 to 29 psig. One curve represents pressure recovery just short of the resonant effect. The second represents pressure recovery for the completely closed valve.

Output flow as a function of pressure recovery is shown in figure 20. The output flow was measured by a flowmeter. Since the flowmeter exhausted into the atmosphere, it read mass flow directly. This mass flow is transformed back to volumetric flow at the pressure existing in the tank at the output of the system assuming an isothermal process, and the output power P is given by

$$P = pQ$$

$$p_1 Q_1 = \frac{p_2}{p_{1_{(abs)}}} \, p_{1_{(gauge)}} Q_2 \tag{1}$$

where p_1 is the gauge pressure of the air in the tank (fig. 18). The pressure $p_{1_{(abs)}}$ appearing in the ratio is a density correction since the flow Q_2 is measured with reference to the atmosphere. The p_2 is the ambient pressure (absolute). In relation (1) we have assumed an isothermal process, hence

$$\frac{\rho_2}{\rho_1} = \frac{p_2}{p_{1_{(abs)}}}$$

where

ρ_2 = density at ambient air pressure

ρ_1 = density at pressure p_1

The maximum power output has been plotted against the input pressure in figure 21. It is evident from the graph, that the maximum power output is about a horsepower. By the same method the power input of the system was calculated, and the power efficiency as a function of input pressure is plotted in figure 22. The power efficiency is about 60 percent over the range considered. The losses are due mainly to pressure and flow degradation, because some of the flow goes out of the opposite channel.

The switching power which denotes the rate at which work must be done to detach the stream from the wall and switch it to the next channel was determined from measurements using apparatus at the control input similar to that described at the output (fig. 12 and 18). The flow was measured with a flowmeter whose maximum range was 0.5 scfm. A valve was provided after the flowmeter whereby the flow could be controlled. Following the valve was a small tank with a combination gauge connected to it. The pressure in the tank was measured initially when the valve was closed and then measured a number of times as the valve was opened slowly; in particular at the time when the unit was at the point of switching. The flow at switching was also measured. Hence, the instantaneous power to switch is defined as

$$p_1 Q_1 = \frac{p_2}{\Delta p_{1(abs)}} p_{1(gauge)} Q_2 \qquad (2)$$

This power was that which passed out of the small needle valve at the instant of switching. In order to calculate the real instantaneous switching power, it would have been necessary to know the total pressure at the output of the control nozzle at the instant of switching, which was not possible. But if it is assumed that the losses from the valve to the nozzle were very small and that the density of the gas did not change significantly, then the switching power calculated is close to the correct one. In equation (2), p_1 is the gauge pressure at the instant of switching, while Δp_1 appearing in the ratio is the difference between the pressure existing in the tank before the valve is open and the pressure in the tank at the instant of flipping. In this case, the source of power is the atmosphere. Since the pressure in the tank is below atmospheric, when the valve is opened, the pressure difference between p_1 and ambient is enough to create the flow necessary to switch the system. It is also possible to obtain switching power for the controls from a supply line through a regulator.

Switching power as a function of supply pressure is shown in figures 23 and 24. From these curves, it is evident that little power is needed to switch the system operating up to 15 psig. The

switching power is only a very small fraction of a watt. Using the power output (fig. 21) and the switching power (fig. 23) the instantaneous power gain may be calculated. It increases rapidly and is about 9,000 at 15 psig. The plot of power gain against input pressure is shown in figure 25. The whole system has a flow capacity of 64 scfm at 15 psig (fig. 26). The flow gain of the system, i.e., the output flow Q_{OUT} divided by the switching flow Q_{CRS}, increases rapidly with supply pressure (fig. 27) until it reaches maximum (3,000) at about 8 psig and then drops slowly as the pressure is increased to 15 psig. The switching flow normalized in terms of the output flow is shown in figure 28. This shows that the relative flow to switch the whole system decreases rapidly up to about 6 psig and then remains essentially constant up to 15 psig.

4. CONCLUSION

It has been shown that digital elements can be cascaded to obtain high-pressure recovery, high flow amplification, and high power gains. This was accomplished by staging three digital elements varying in nozzle areas by a factor of 10. The design of the system was arrived at by testing single units and then matching them until stable operation over a particular range was possible. The problem encountered in the matching process was that feedback loops arise between units in the region of no flow. These feedback loops must be controlled to obtain stable operation.

The third stage was operated in the subsonic range up to 15 psig. The flow gain was about 3,000, the power gain increased steadily up to 10,000, and the flow output was 64 scfm at 15 psig. The operation of staged units is characterized by large noise outputs. The noise arises from interaction of the main stream with the splitters. Their physical nature may be of the edge-tone type combined with background noise that arises through friction. The oscillations are decreased by rounding the wedge, which reduces some of the modes of acoustic frequency oscillation associated with the jet-edge system.

5. FURTHER PROBLEMS

More research is necessary to develop analytic design methods that can be correlated with experimental results, including the following: measurement of pressure profiles before entrance into a diffuser; measurements of static pressure profiles along the boundaries of the amplifier; and reduction of acoustic noise generated in jet-edge oscillations.

ACKNOWLEDGMENT

The author is greatly indebted to Raymond Warren for his advice and supervision in the process of this work and to Leon Katchen for his cooperation in obtaining the data.

6. REFERENCES

(1) Borque and B. C. Newman, Aeronautical Quarterly, Vol XI, August 1960.

(2) M. L. Albertson, Amer. Soc. of Civil Eng., Paper No. 2409.

(3) C. Sondhaus, Ann. Phys. Lpz., 91, 128 and 214 (1854).

(4) R. Wachsmuth, Ann. Phys. Lpz., 14, 469 (1904).

7. BIBLIOGRAPHY

R. E. Olson, "Studies of Pure Pneumatic Elements," United Aircraft Corporation, DOFL Contract No. DA-49-186-ORD-512, 28 June 1961.

F. T. Brown, Sc. D. Thesis, MIT, Dept of Mech. Eng., May 1962.

C. B. Brown, Proc. Phys. Soc. (London) 49, 493 (1937)

Lighthill, M. J., "Notes on the Deflection of Jets by Insertion of Curved Surfaces," R.M. 2105, 1945.

Glauert, M. B., "The Wall Jet," Journal of Fluid Mech., Vol 1, 1956.

Schlichting, H., Boundary-Layer Theory," 4th Edition, McGraw-Hill Book Co., Inc., N. Y., 1960 p 605.

Sawyer, R. A., "The Flow Due to a Two-Dimensional Jet Issuing Parallel to Flat Plate," Journal of Fluid Mech., Vol 9, Part 4, Dec. 1960.

A. B. Bailey, "Use of Coanda Effect for the Deflection of Jet Sheets over Smoothly Curved Surfaces," UTIA Technical Note No. 49, Part I and II.

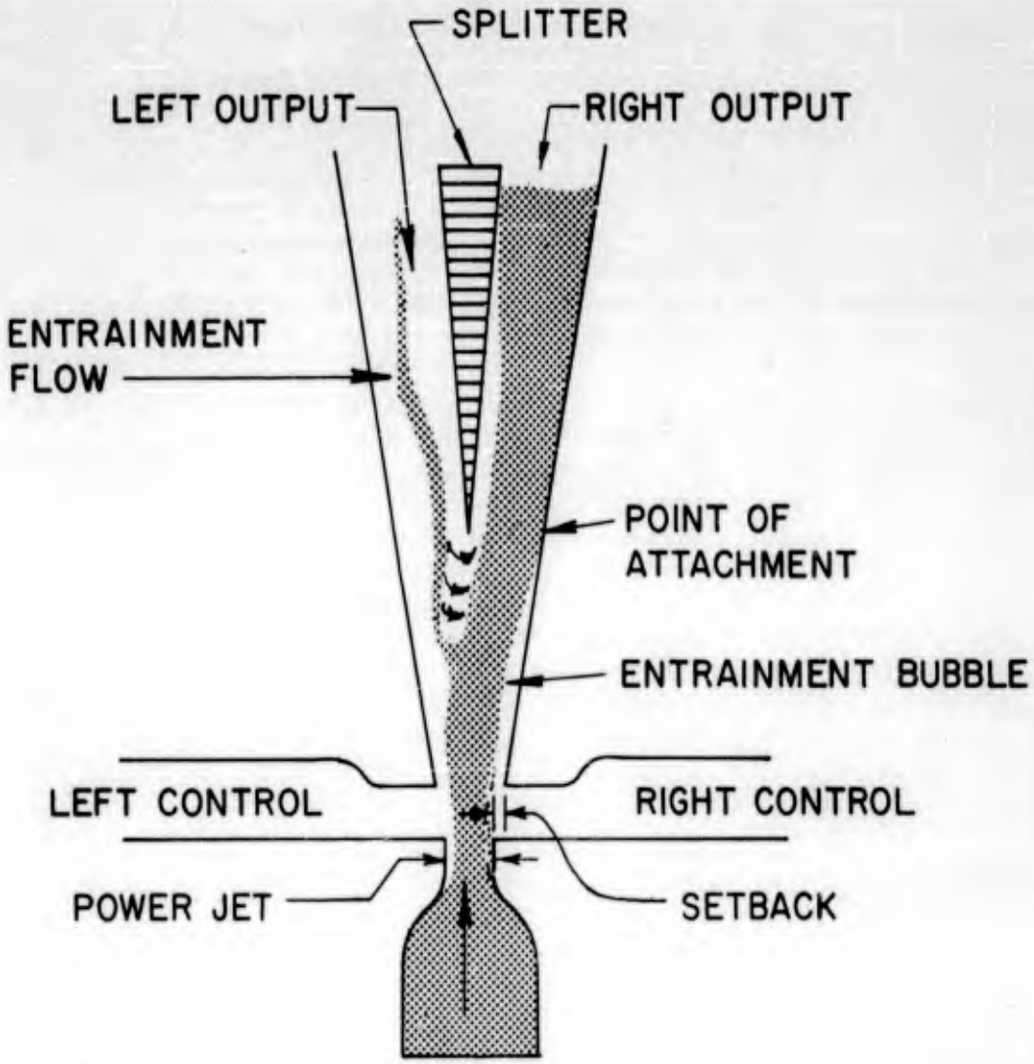

Figure 1. Schematic diagram of fluid flow in a boundary-layer digital unit.

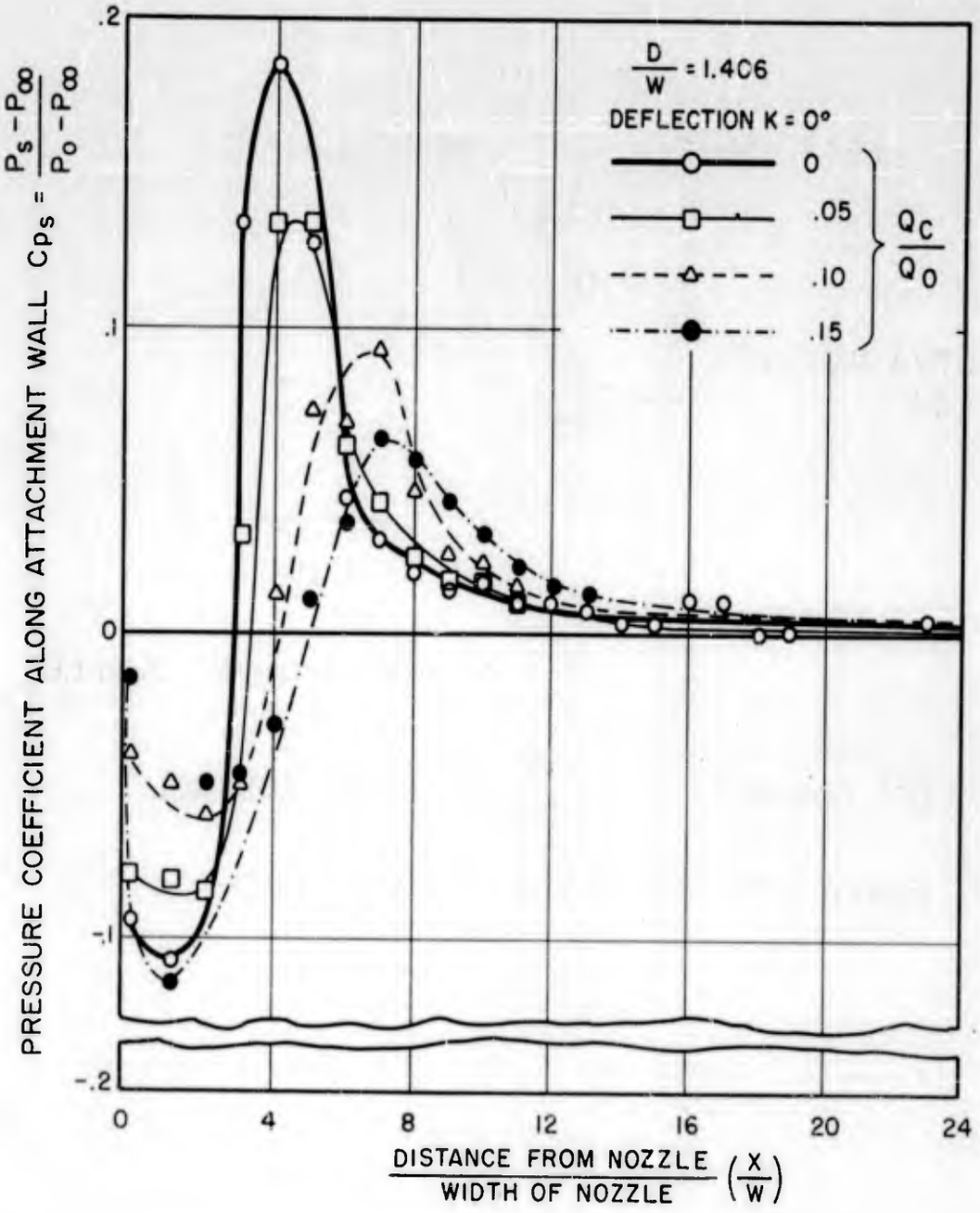

Figure 2. Pressure distribution along the attachment wall. Q_c = control volumetric flow rate; Q_o = power-jet volumetric flow rate at nozzle exist; D = setback; K = wall inclination angle; X = distance along attachment wall; P_s = static pressure of power-jet supply; P_∞ = ambient pressure; and w = nozzle width.

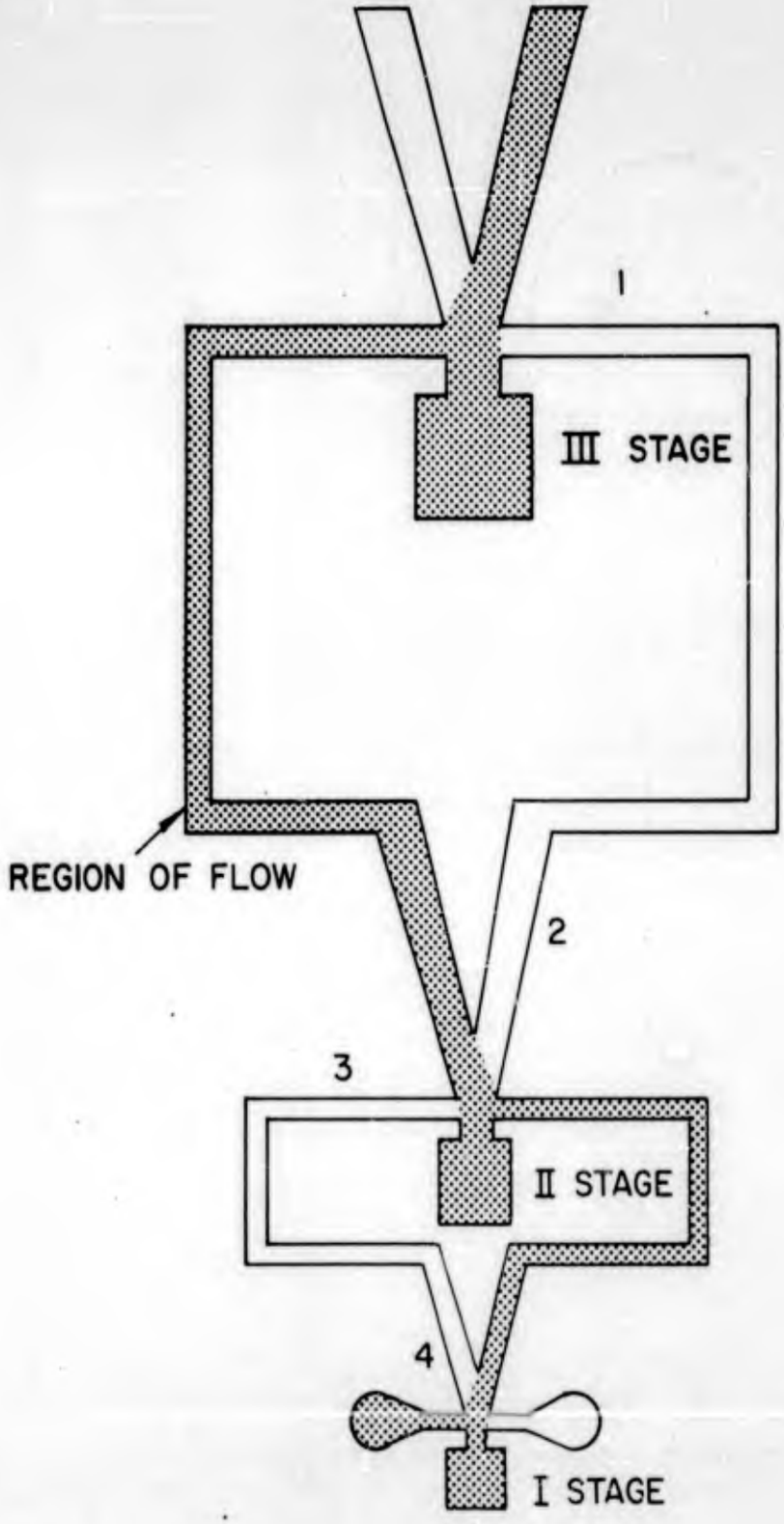

Figure 3. Schematic diagram of three-stage digital amplifier.

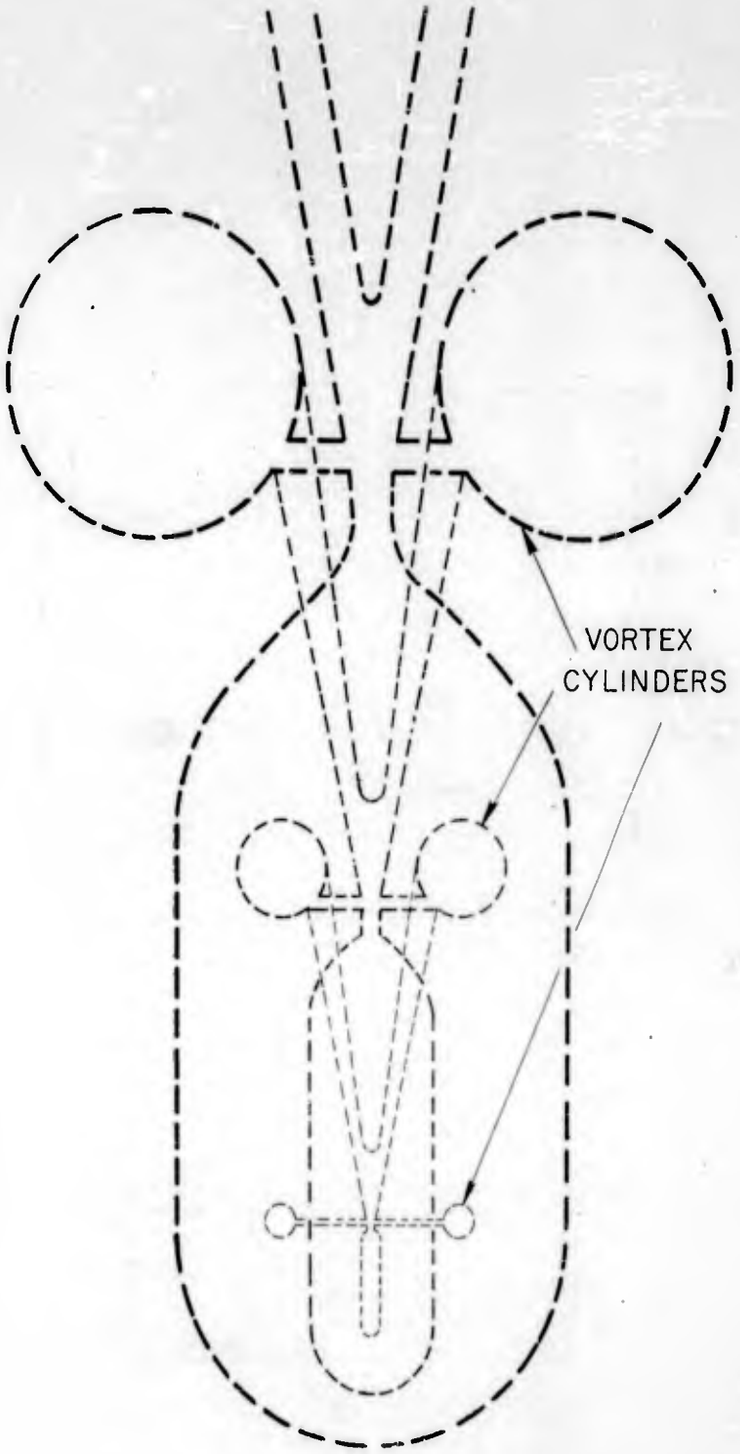

Figure 4. Integral three-stage digital amplifier.

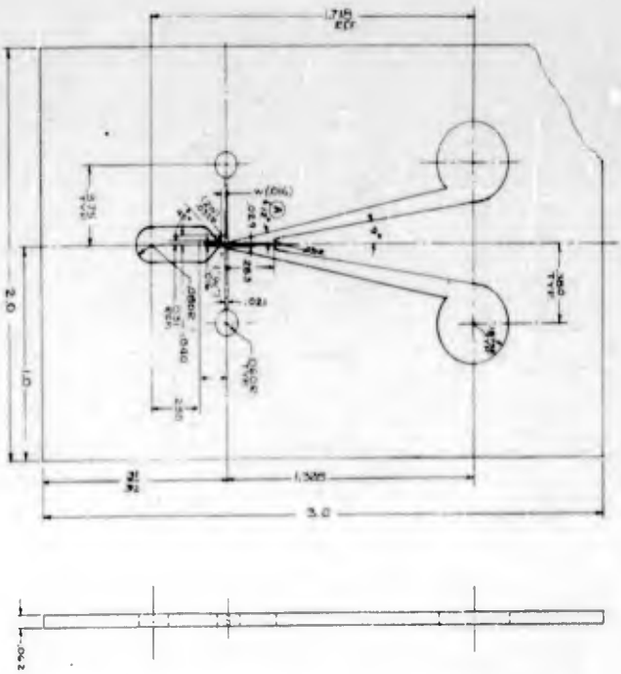

Figure 5. Aluminum first stage of integral digital amplifier—design drawing.

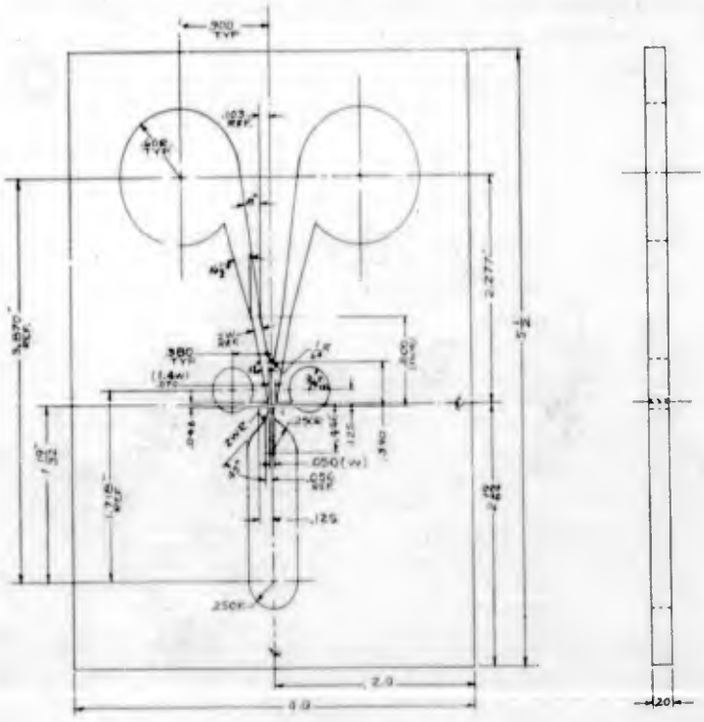

Figure 6. Aluminum second stage of integral digital amplifier—design drawing.

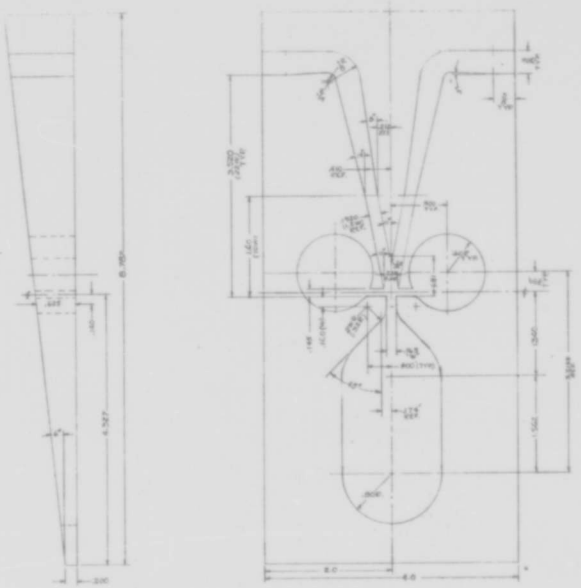

Figure 7. Aluminum third stage of integral digital amplifier—design drawing.

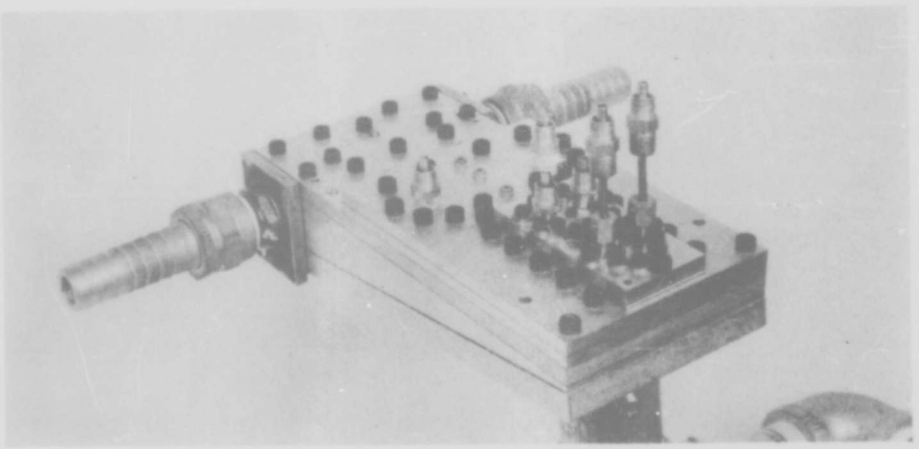

Figure 8. Integral three-stage digital amplifier.

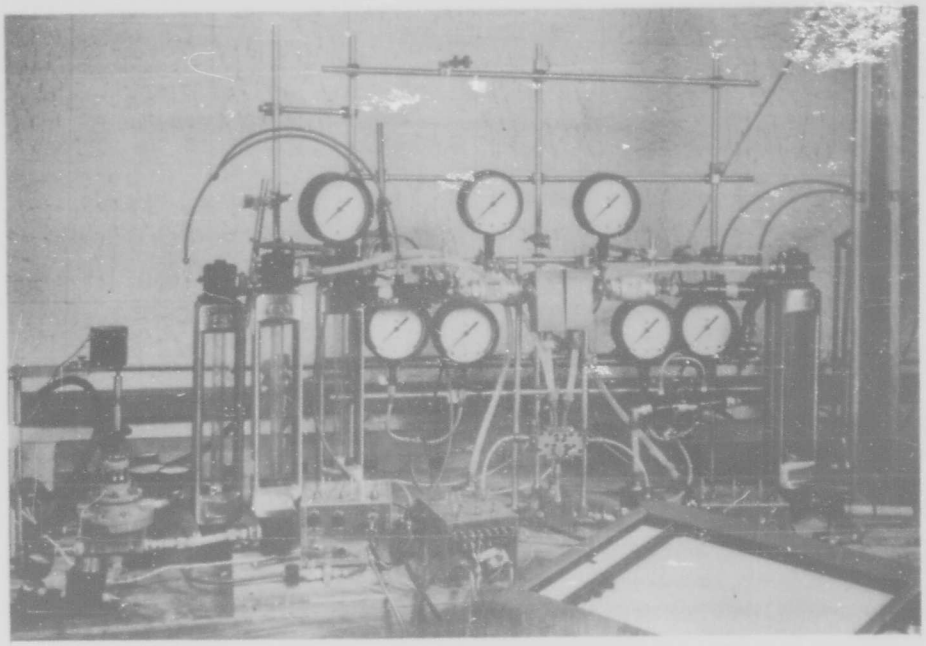

Figure 9. Apparatus for testing single digital elements.

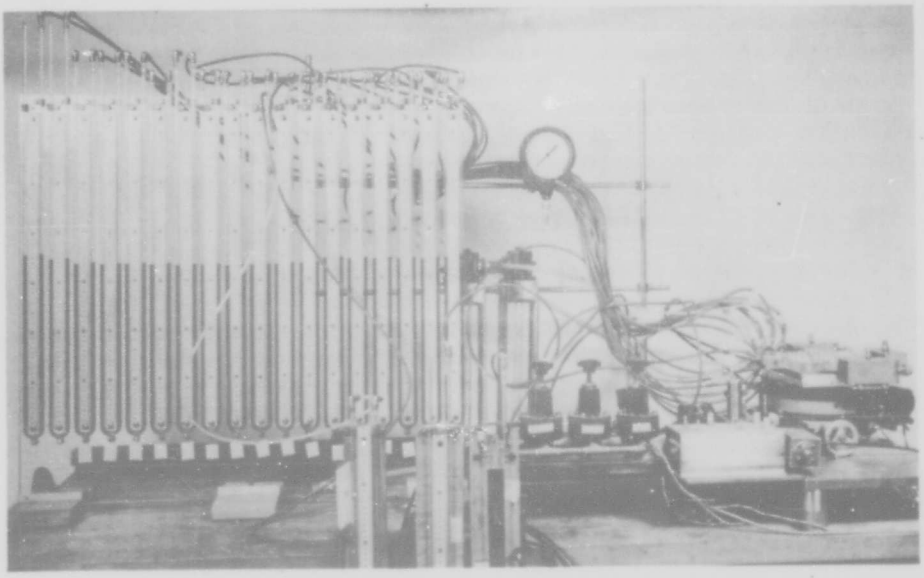

Figure 10. Apparatus for measuring pressure distribution on attachment wall.

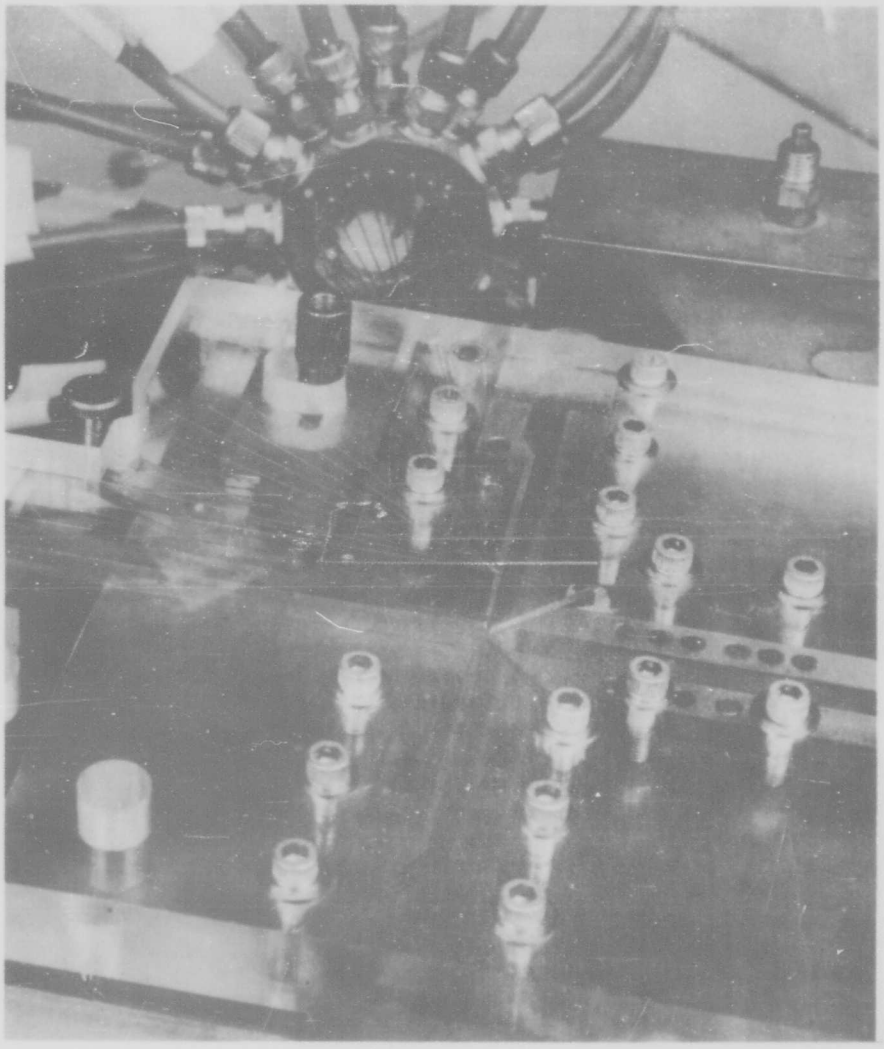

Figure 11. Instrumentation of digital element for pressure-distribution measurements.

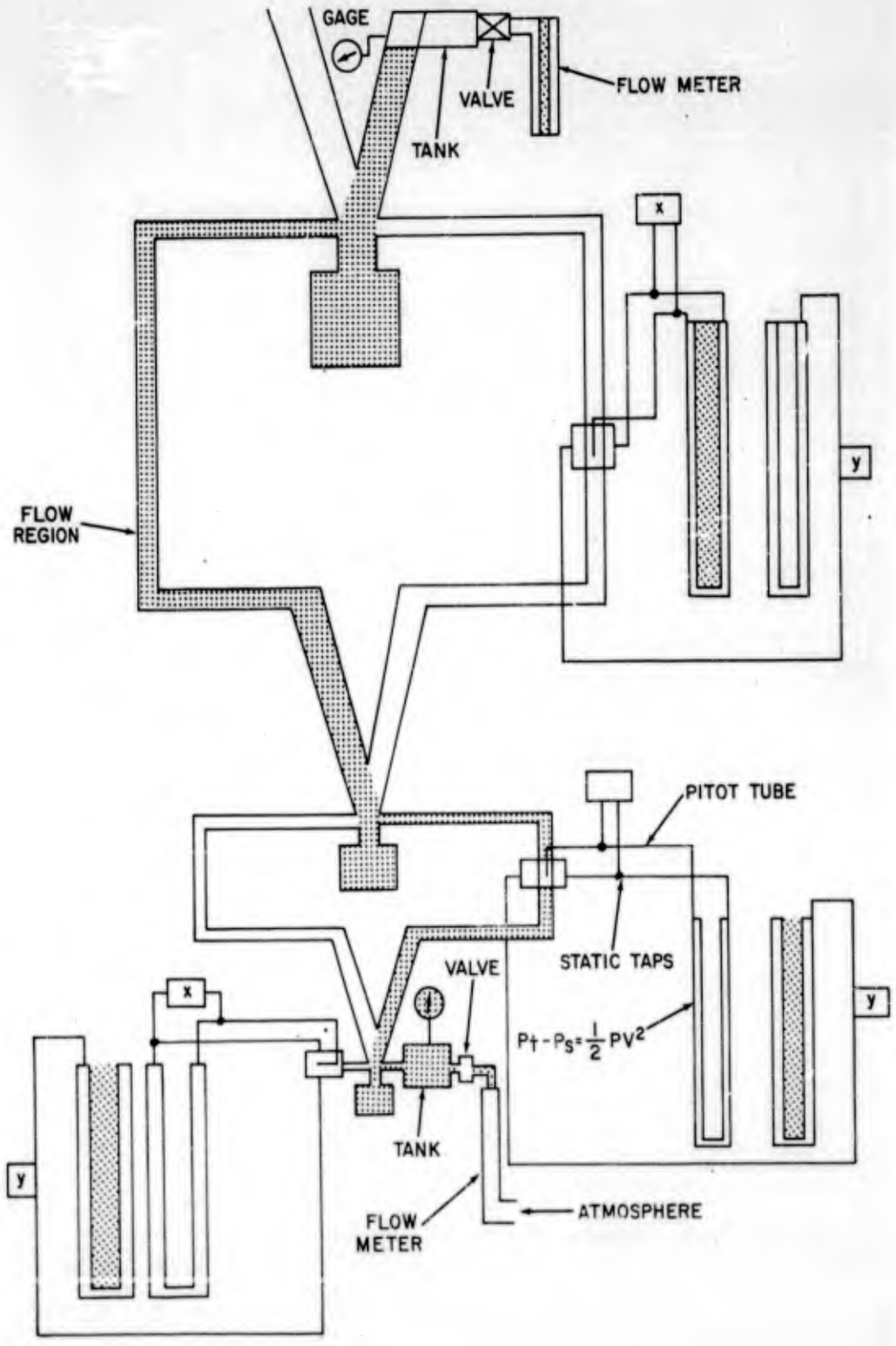

Figure 12. Schematic of apparatus for testing three-unit digital amplifier system.

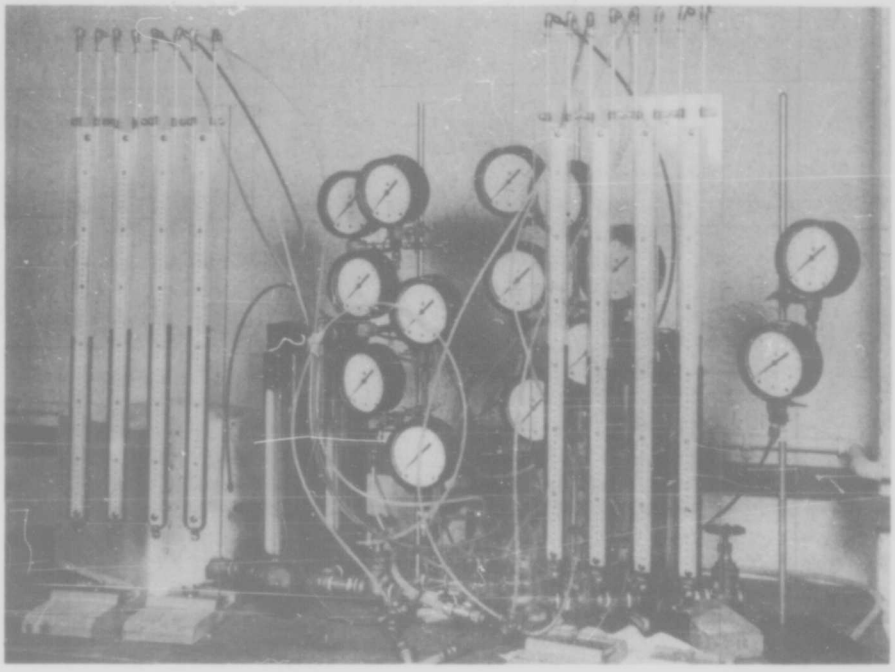

Figure 13. Apparatus for testing three-unit digital amplifier system.

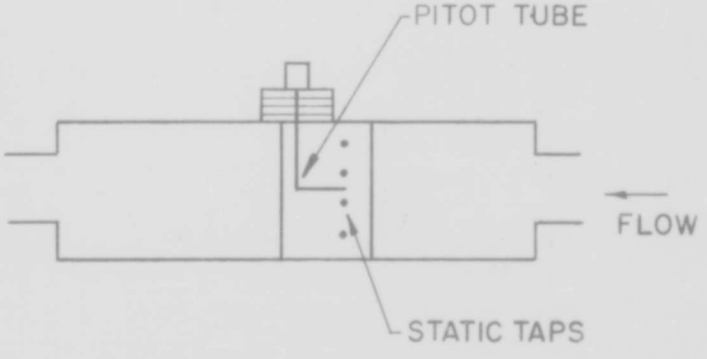

Figure 14. Instrumentation for measuring output pressures.

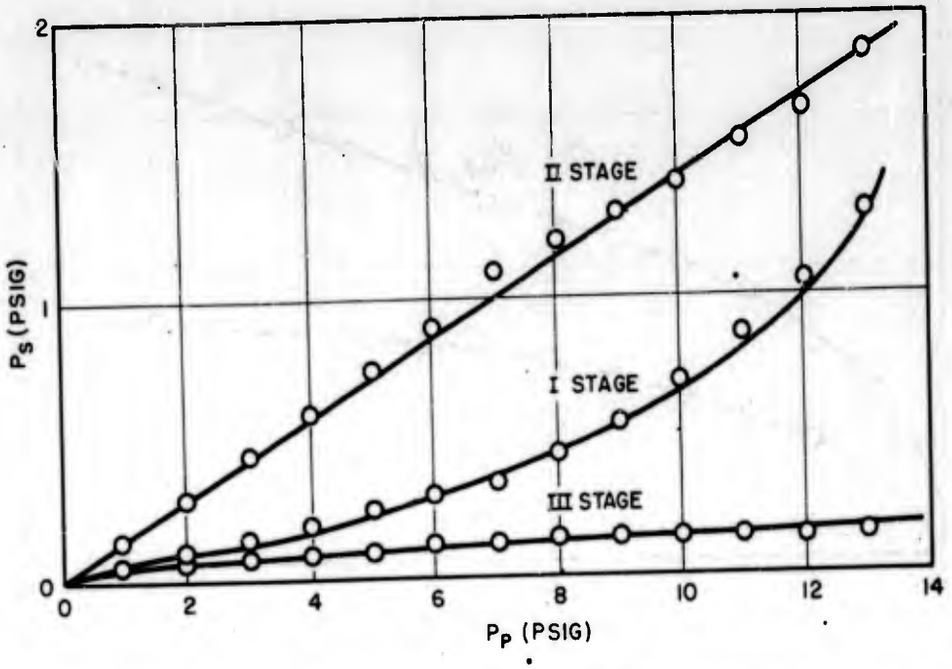

Figure 15. Static pressure in flow region of three-unit digital amplifier versus power-jet supply pressure

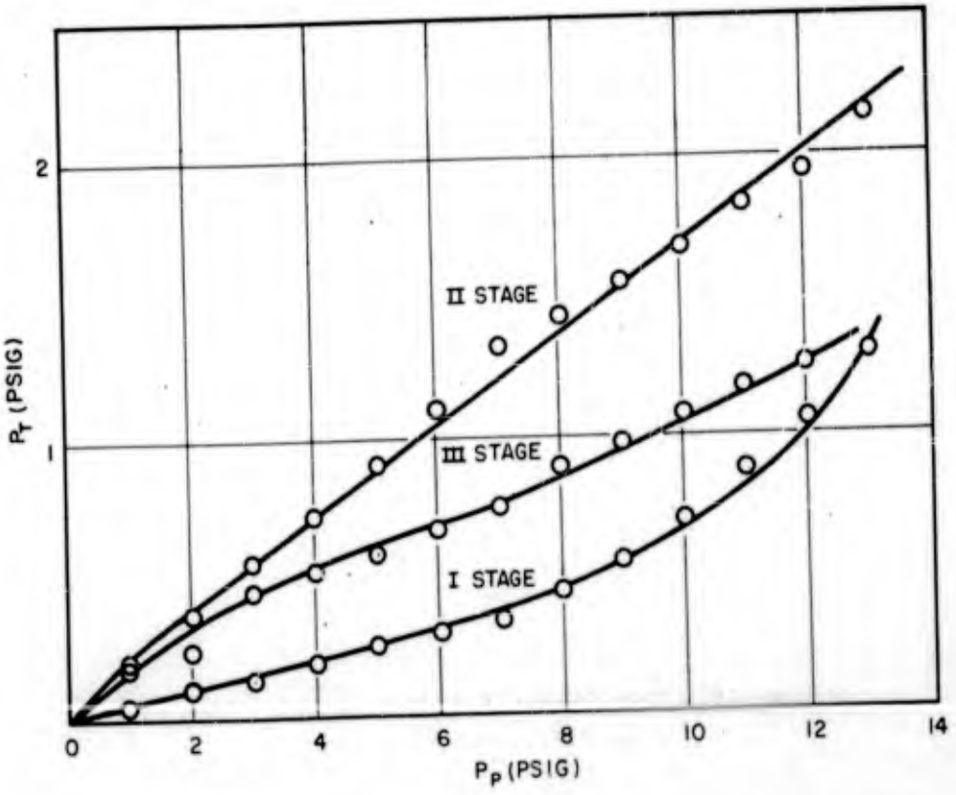

Figure 16. Total pressure in flow region of three-unit system versus power-jet supply pressure.

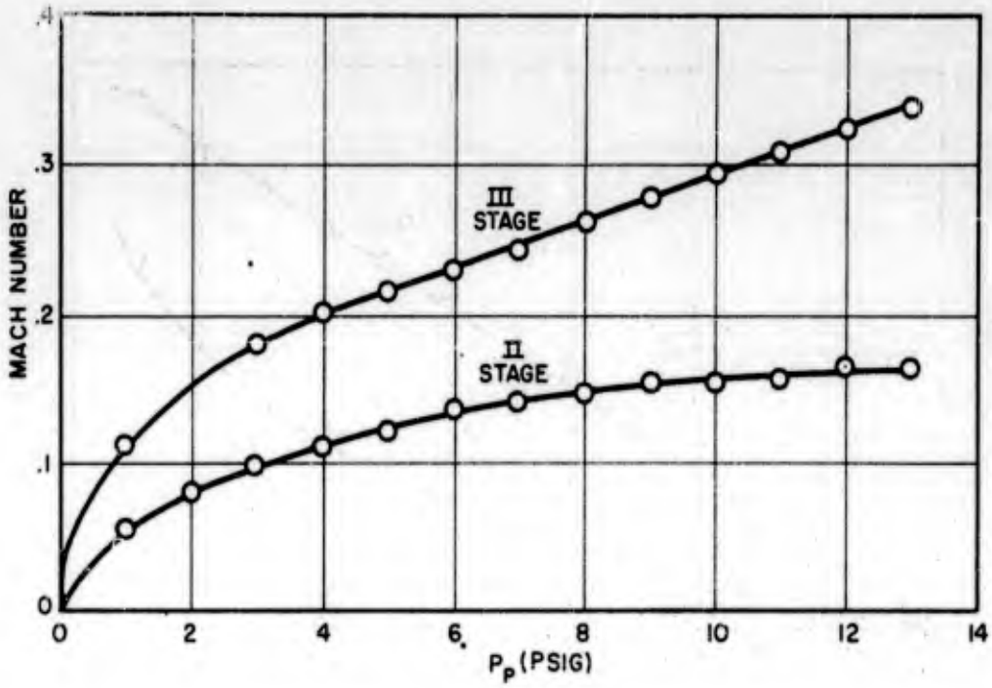

Figure 17. Mach number in three-unit digital amplifier system versus power-jet supply pressure.

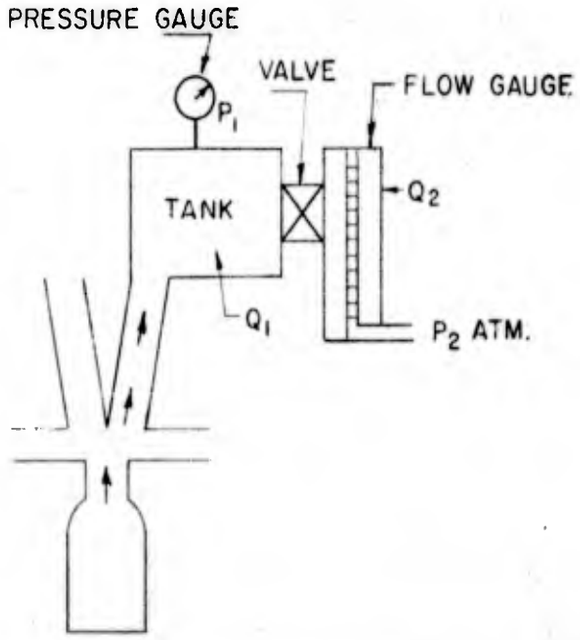

Figure 18. Instrumentation for measuring output flow and pressure.

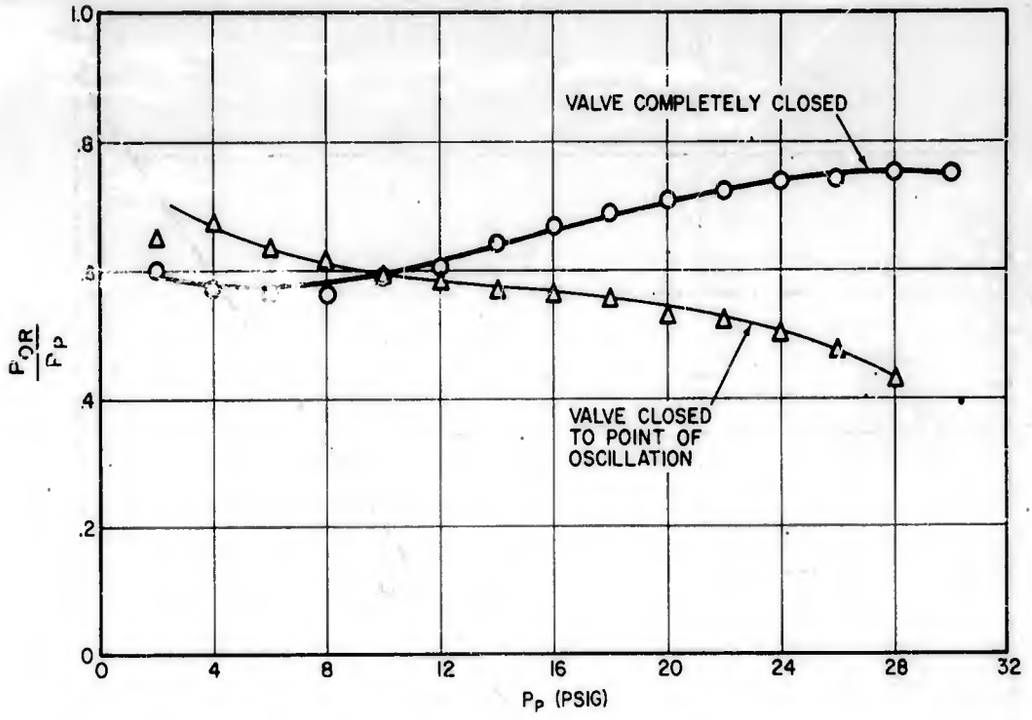

Figure 19. Pressure recovery in integral three-stage digital amplifier versus power-jet pressure.

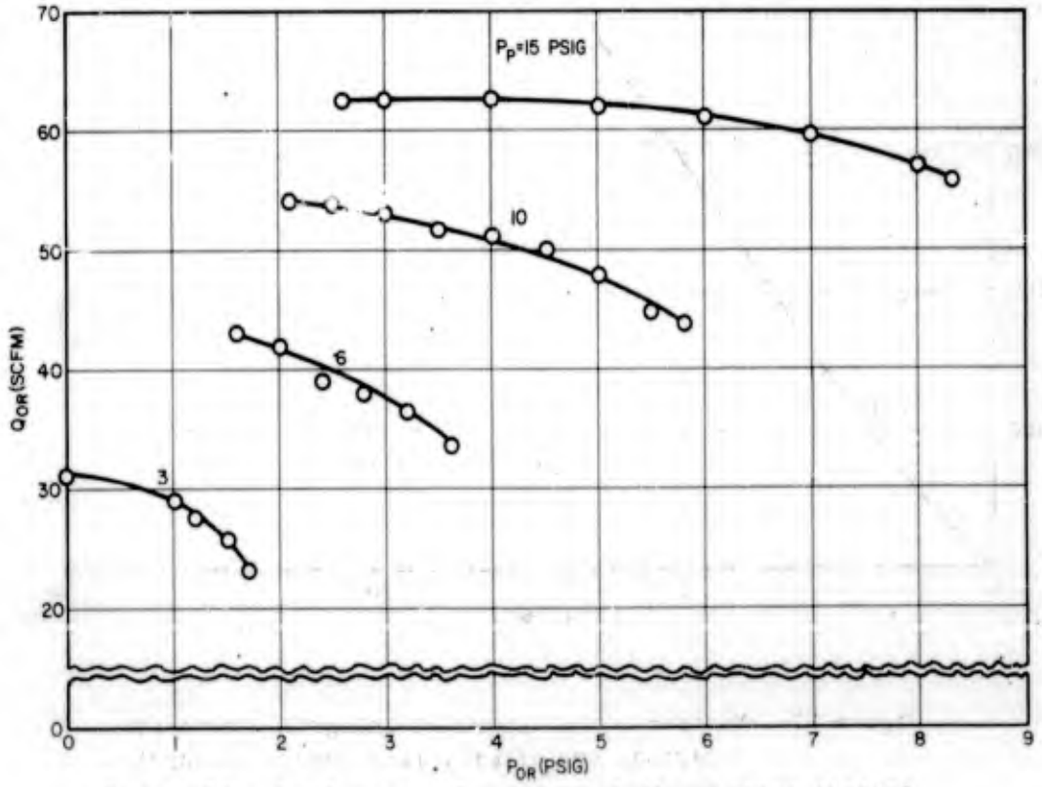

Figure 20. Load curves for integral three-stage digital amplifier.

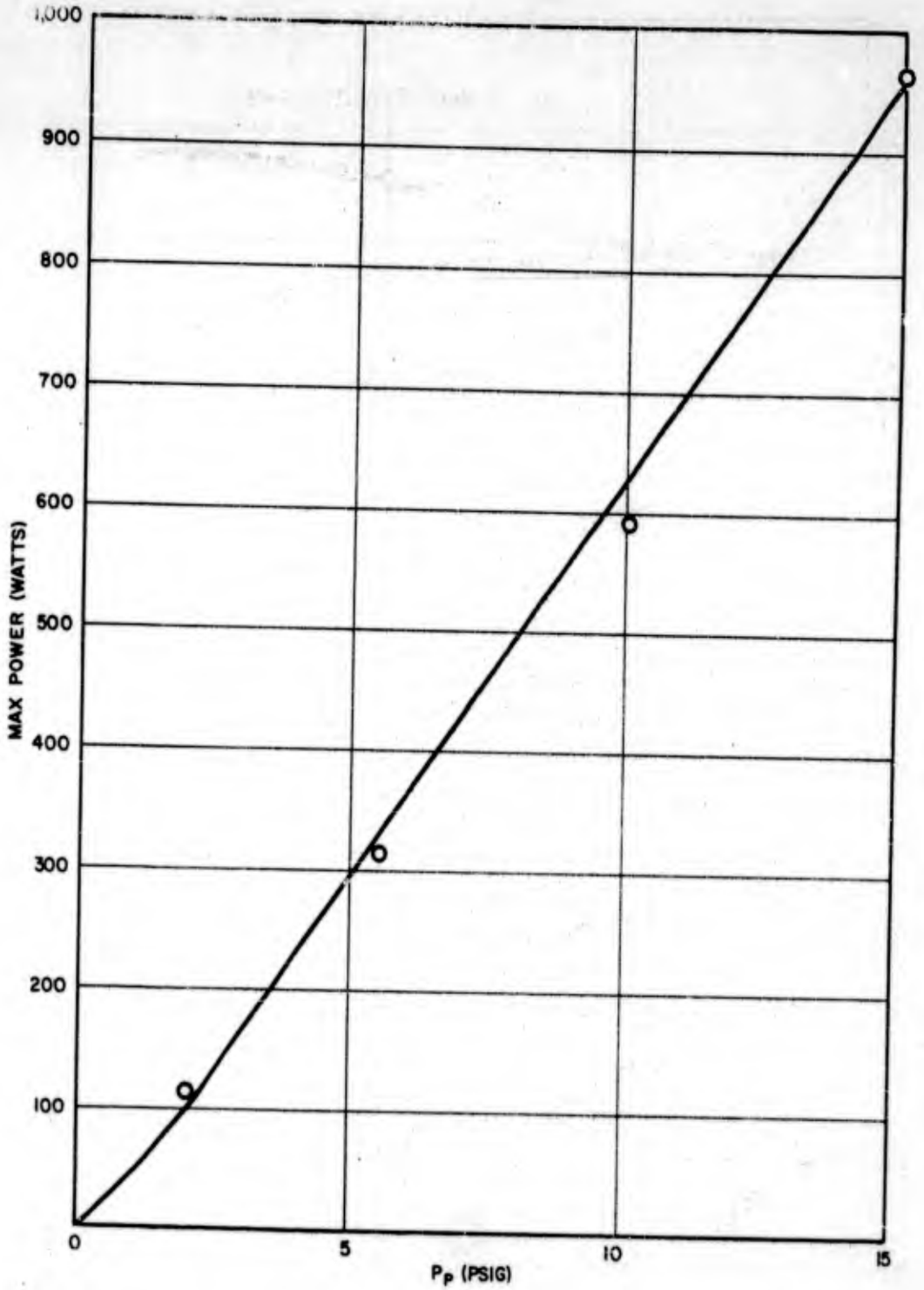

Figure 21. Maximum output power of integral three-stage digital amplifier versus power-jet supply pressure.

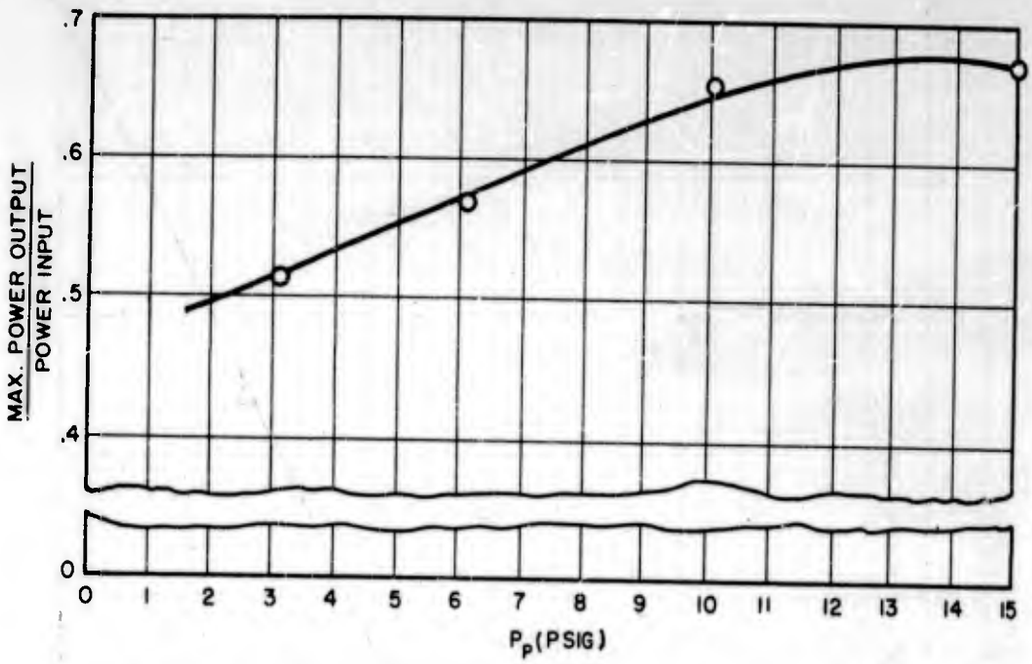

Figure 22. Power efficiency of integral three-stage digital amplifier versus power-jet supply pressure.

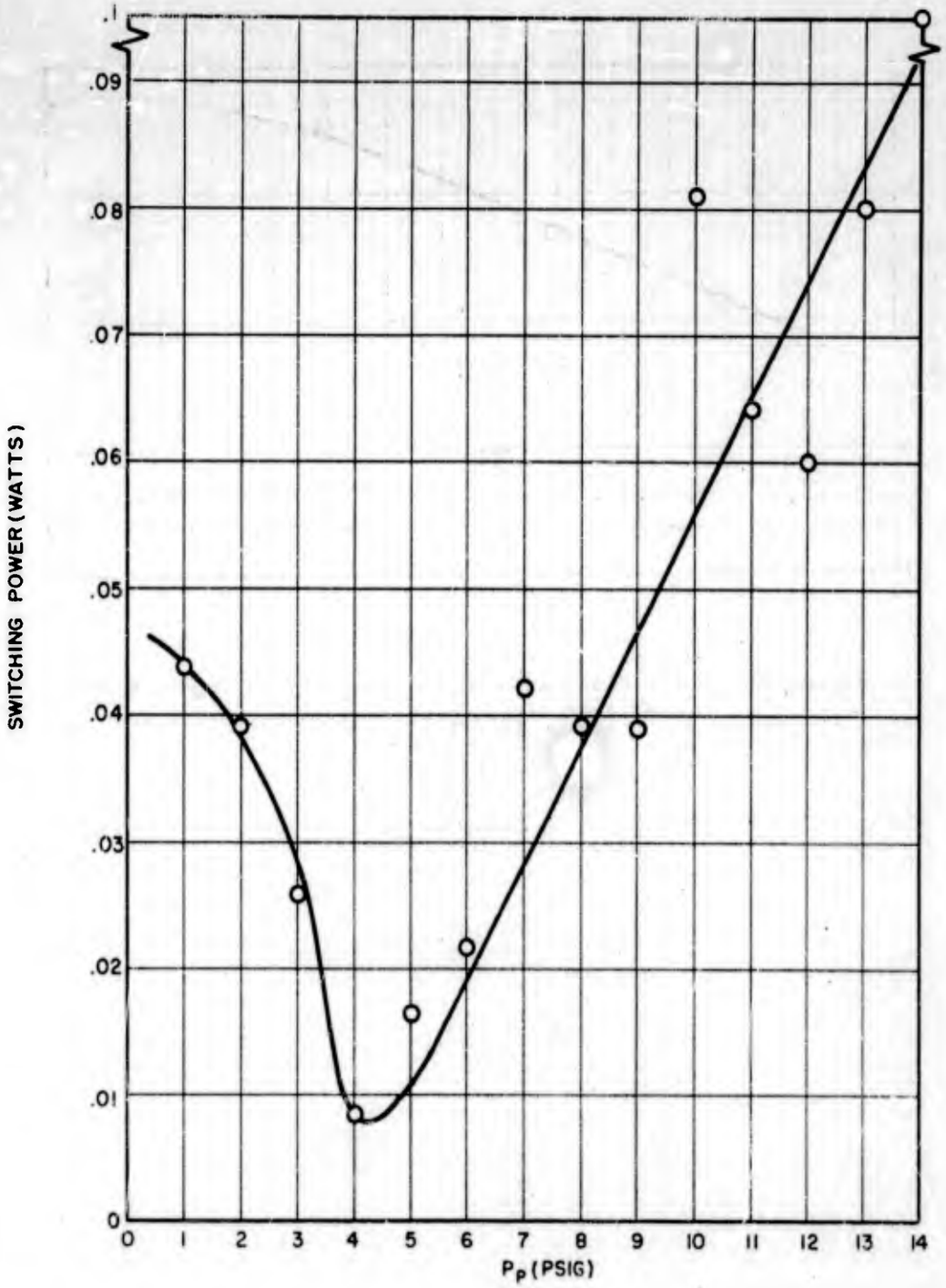

Figure 23. Switching power (watts) of integral three-stage digital amplifier versus power-jet supply pressure.

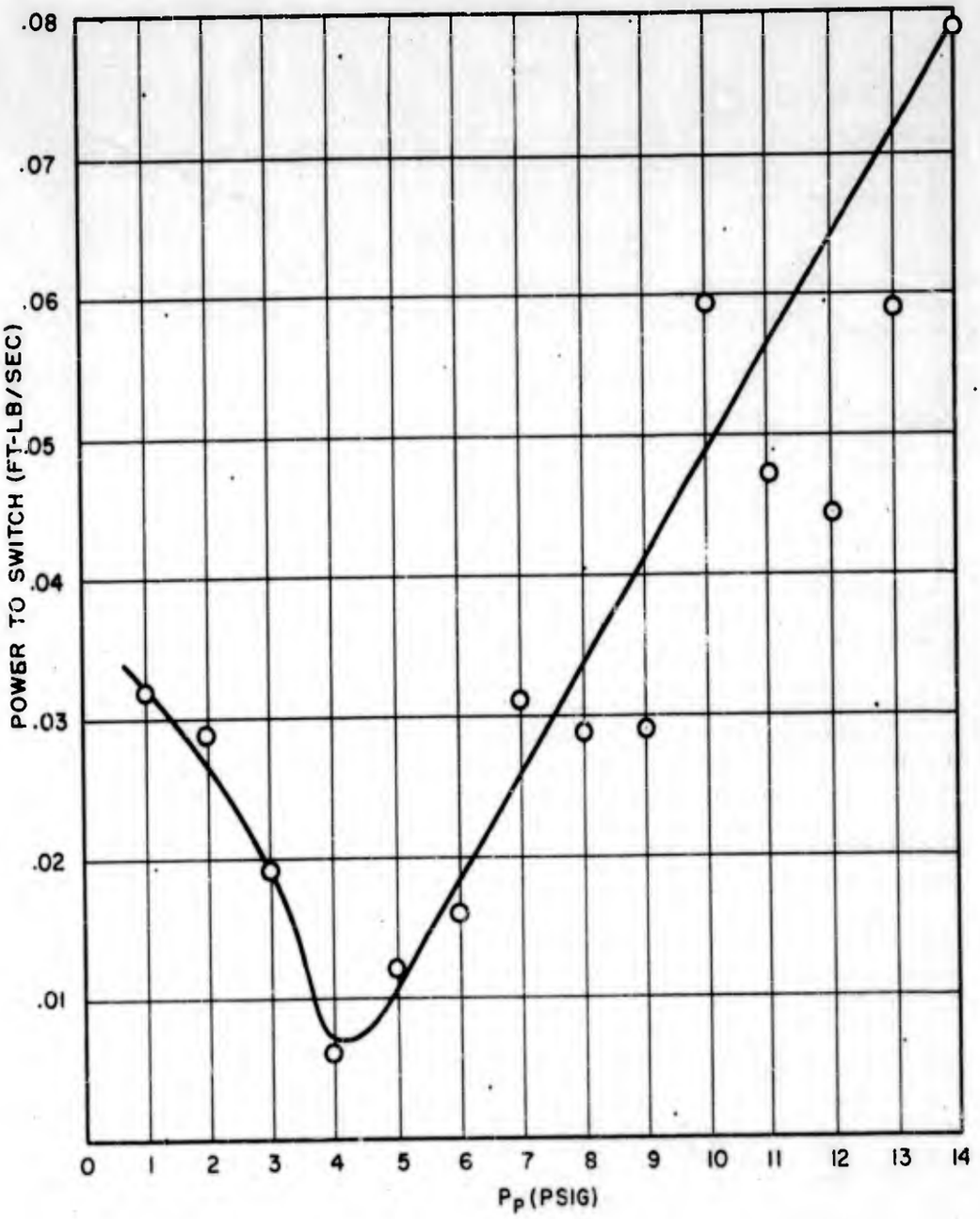

Figure 24. Switching power (ft-lb/sec) of integral three-stage digital amplifier versus power-jet supply pressure.

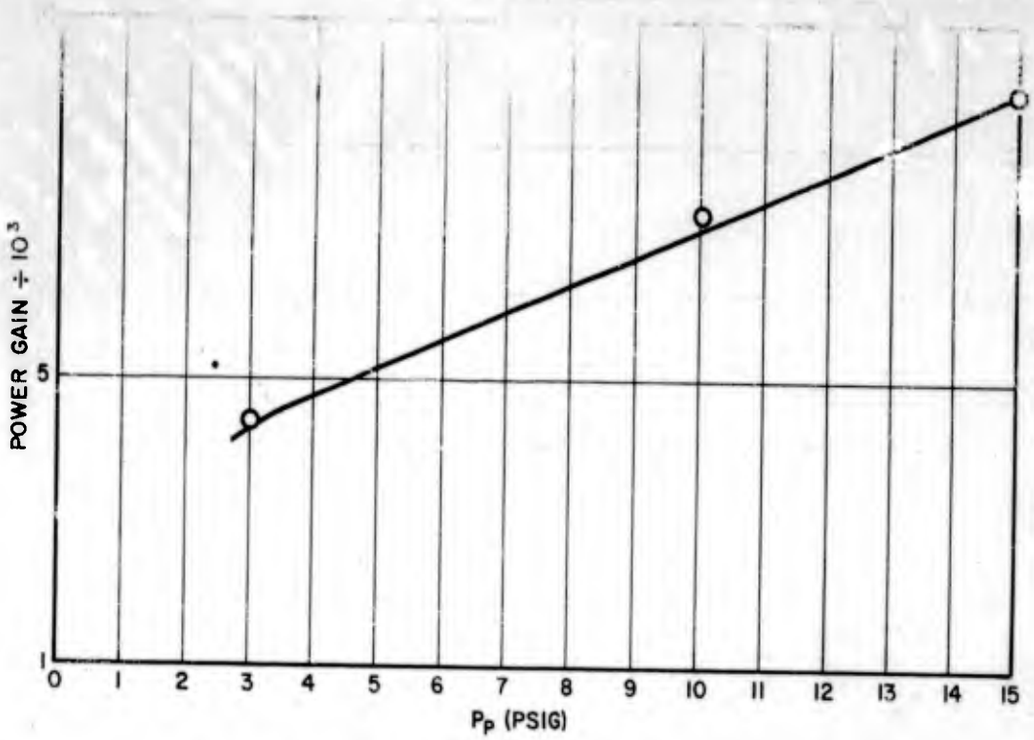

Figure 25. Instantaneous power gain of three-stage digital amplifier versus power-jet supply pressure.

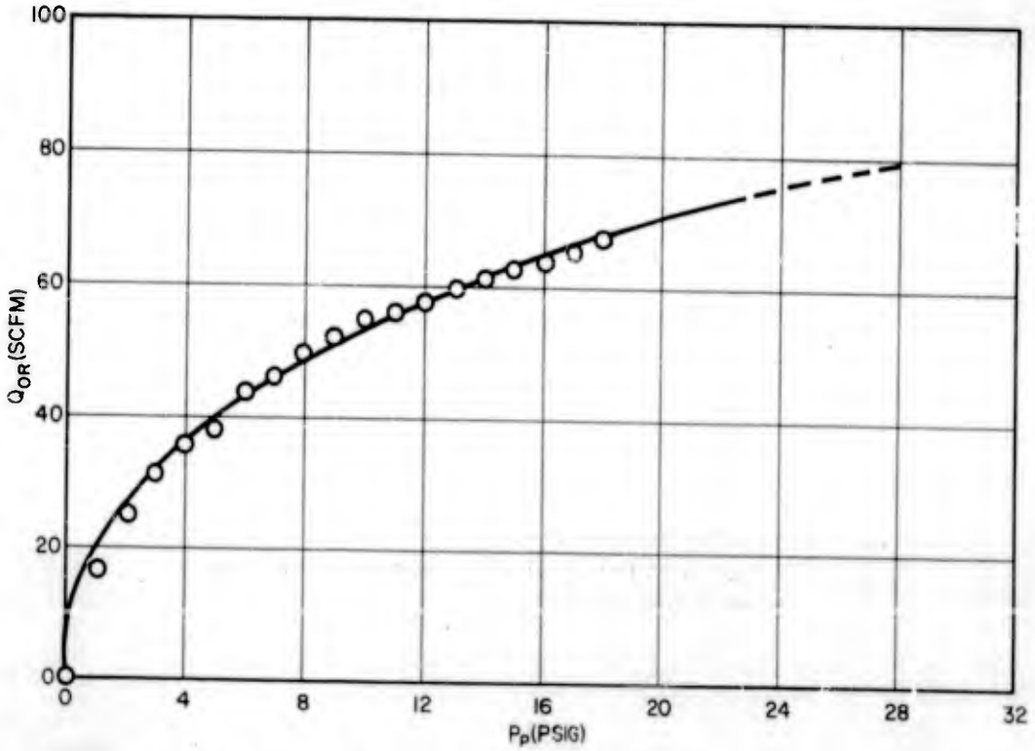

Figure 26. Output flow versus power-jet supply pressure for integral three-stage digital amplifier.

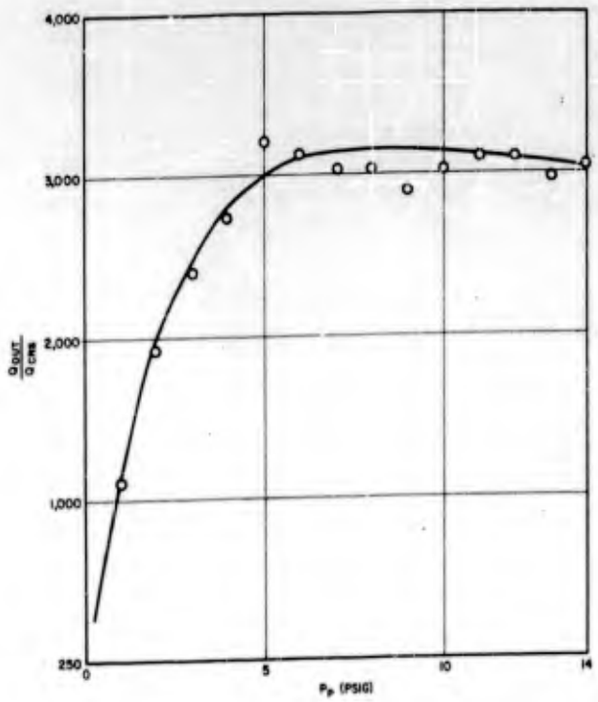

Figure 27. Flow gain of integral three-stage digital amplifier versus power-jet supply pressure.

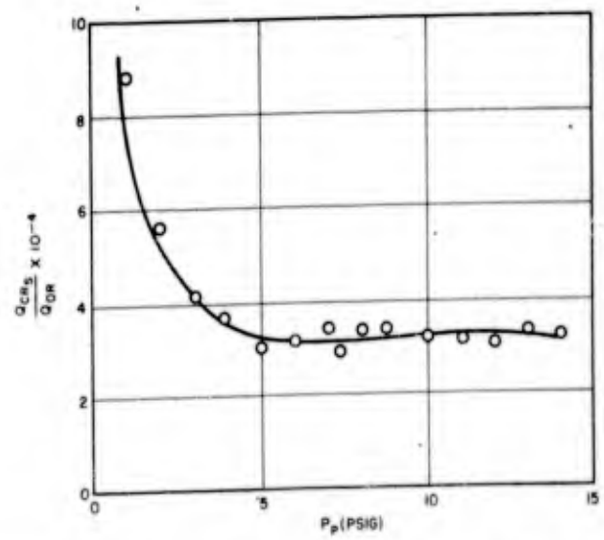

Figure 28. Normalized switching flow for integral three-stage digital amplifier versus power-jet supply pressure.

UNCLASSIFIED